J. Biomechanics Vol. 23, No. 6, pp. 589–595, 1990.
Printed in Great Britain

0021-9290/90 $3.00 + .00

THREE-DIMENSIONAL OSSEO-LIGAMENTOUS MODEL OF THE THORAX REPRESENTING INITIATION OF SCOLIOSIS BY ASYMMETRIC GROWTH

IAN A. F. STOKES and JEFFREY P. LAIBLE

Department of Orthopaedics and Rehabilitation and Department of Civil and Mechanical Engineering, University of Vermont, Burlington, VT 05405, U.S.A.

Abstract—A biomechanical model of the human thorax was constructed to investigate how asymmetric growth of the thorax might initiate spinal lateral curvature and axial rotation as seen in scoliosis deformities. Geometric data specifying nodal points of the model were taken from stereo-radiographs of an adolescent subject. An initially symmetrical geometry was created by 'mirroring' measurements of a hemi-thorax and spine. Published data provided cross-sectional measurements of the ribs, material properties of tissues and global flexibilities of the intervertebral motion segments. The ribs, sternum, intervertebral motion segments and intercostal ligaments were represented by elastic elements. Model deformations were calculated by the direct stiffness finite element method, with growth represented by an initial strain term in the constitutive law. Non-linear behavior was accommodated by running the model recursively, with updated node locations at each step. Both stress relaxation and stress modulation of growth in the component tissues were simulated. Thoracic growth of 20% with asymmetric growth of the ribs was simulated to give rib length asymmetries of 11%, similar to that observed in a previous study of patients with idiopathic scoliosis. This resulted in the model having a small thoracic scoliosis curvature convex toward the side of the longer ribs. Variations of the model which permitted free motion at the costo-vertebral joints or produced changes in the curvature of the posterior parts of the ribs resulted in axial rotation of the vertebrae similar to that observed clinically. The model supports the idea that growth asymmetry could initiate a small scoliosis during adolescence.

INTRODUCTION

This paper describes a structural model of the human thorax and its use in simulating the effects of growth in relationship to etiology of idiopathic scoliosis. Idiopathic scoliosis is a deformity which develops during a period of rapid growth. The rate of progression during growth can exceed $5^\circ\,yr^{-1}$, and reduces to typically $0.3^\circ\,yr^{-1}$ in larger curves after skeletal maturity (Weinstein and Ponseti, 1983). There is also evidence of asymmetric growh of the vertebrae being responsible for causing scoliosis (Roaf, 1963). More general asymmetric growth was implicated by Dangerfield *et al.* (1980) who reported that the upper arm lengths of subjects with thoracic scoliosis were longer on the right side, compared with a control group without scoliosis. We have found (Stokes *et al.*, 1989) a tendency for the rib lengths of patients with scoliosis to be asymmetric. Patients with single right thoracic scoliosis tended to have longer ribs on the right side. Those with single left lumbar curves tended to have longer ribs on the left side. Those with double curves generally had longer ribs on the left side. Agadir *et al.* (1988) reported scoliosis in an animal model associated with rib growth asymmetry produced by intercostal nerve resection.

These observations of asymmetries of the thorax and upper arms implicate asymmetric growth in etiology of scoliosis; however, they do not establish that asymmetric growth is the primary cause of the spinal and other asymmetries, nor do they define the precise kinematic and kinetic mechanisms reponsible for the observed changes. These biomechanical aspects of curve development were analysed by finite element modelling techniques. These techniques are suitable for analysing problems with complex geometry and material properties.

This paper presents a finite element osseo-ligamentous structural model of the human thorax, and its behavior with inputs representing asymmetrical growth in order to examine the hypothesis that asymmetric growth of the rib cage might initiate the scoliosis deformity. The effects of varying distribution of growth, flexibility of costo-vertebral joints, stress–growth interactions, and the end constraints were investigated. The output of each model was examined for spinal symmetry measured by the Cobb angle, and by the vertebral axial rotation.

METHODS

Geometric data

Nodal point coordinates were obtained from stereo-radiographic reconstructions of the ribs and vertebrae of living subjects (Dansereau and Stokes, 1988; Stokes *et al.*, 1989). This method provided the Cartesian coordinates of six landmarks on each vertebra (vertebral endplates and bases of pedicles), 60 equally spaced points along the midline of each rib, and coordinates of the costo–sternal articulations. From these coordinates the geometry of each thoracic vertebra was defined by six nodal points representing the vertebral body center, the transverse processes, the rib head–vertebra articulation and the spinous process.

Received in final form 17 *October* 1989.

Each lumbar vertebra was represented by four nodal points (vertebral body center, transverse processes and spinous processes); the bony part of each rib was represented by 11 nodal points and a further 28 points defined the costal cartilages and sternum. Since two points on each rib were co-incident with two of the thoracic vertebral nodes, a total of 336 nodal points defined the overall shape of the model (Fig. 1).

The initial geometry was taken from one of a group of patients with scoliosis previously measured by stereo radiography (Stokes *et al.*, 1989). The measurements of a 13-yr-old female with a single lumbar scoliosis of 24° Cobb and no thoracic structural curve were selected as representative of the shape of the adolescent thorax. Then an idealized symmetric model was created by reflecting the geometry of the right side of the thorax to the left side, and also by making the bony parts of the ribs lie in a best fit plane. This symmetrical rib cage was then merged with the spine which had been modified to have no curvature in the frontal plane. This spine was created by taking the sagittal plane projection of the original three-dimensional spine.

Cross-sectional properties of the ribs and costal cartilages were obtained from published measurements (Roberts and Chen, 1972). The principal axes of these cross-sections were aligned in the model by specifying a direction to an additional (third) nodal point. After inspection of articulated skeletal specimens, this third node was specified as a nodal point on an adjacent (cephalad) rib. In the case of the first ribs, the additional nodes were located at the mid points of the chords joining the two ends of the rib.

Based on the nodal point coordinates, the stiffness characteristics of the model were then formulated by making connections between the nodes, using various elements representing anatomical structures. The ribs and sternum were constructed from straight beam elements. Intercostal ligaments (in a crossed formation between adjacent ribs) were represented by spring elements. The vertebral processes were constructed from beams. The intervertebral motion segments were modelled by means of 12×12 stiffness matrix elements. These elements do not represent any particular geometric shape or material properties, but incorporate the published (Panjabi *et al.*, 1976) relationships between the six degrees of freedom of motion of an intervertebral motion segment and the three principal forces and moments applied to them. The stiffness matrices were rotated to align them with the global (model) coordinates of the nodal points representing mid-points of vertebrae.

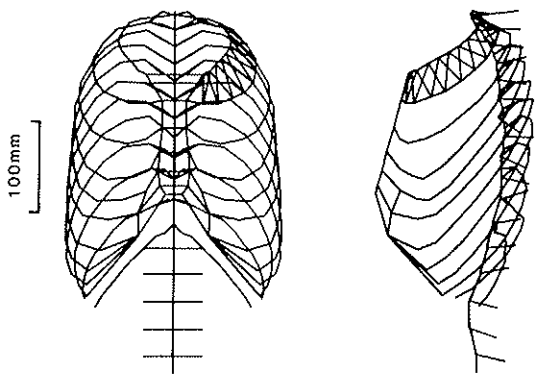

Fig. 1. Initial geometry of the three-dimensional model of the rib cage (frontal and lateral views). Only the intercostal ligaments at T1–T2 ribs on one side have been shown, for clarity.

The costo–central articulations at the articulation of the rib head with the vertebra were modelled as 'ball and socket' joints (without transmission of moments). These joints were considered to be of unifacetal type (Gloobe and Nathan, 1970) having an articulation only with the vertebra at the same anatomical level. The costo–transverse joints were modelled by flexible beam elements. The resulting costo–vertebral articulations then had their lowest stiffness for rotation about the axis of the rib head, the preferred axis reported by Jordanoglou (1969).

Elastic properties

These properties of the model were difficult to obtain, because of the known non-linearity, inhomogeneity, etc., of biological tissues, and because of problems obtaining individualized data from living subjects. All material properties were taken from published data.

Linear elastic properties of the elements representing vertebral processes, the ribs, sternum, ($E = 12.0\,\mathrm{kN\,mm^{-2}}$), and costal cartilages ($E = 0.3\,\mathrm{kN\,mm^{-2}}$) were initially obtained by using the published values of the Young's modulus of rib bone costal cartilage (Roberts and Chen, 1970). In the case of the intercostal ligaments, the value of $E = 25\,\mathrm{N\,mm^{-2}}$ was adopted because it was intermediate between the values given by Fung (1981) for elastin ($E = 0.6\,\mathrm{N\,mm^{-2}}$) and collagen fibers ($E = 1.0\,\mathrm{kN\,mm^{-2}}$).

The experimentally derived (6×6) stiffness matrices reported by Panjabi *et al.* (1976) (average values for the thoracic spine region) were used to create a two-node element with six degrees of freedom per node representing intervertebral motion segments. Equilibrium and compatibility were considered in constructing the 12×12 stiffness matrices for these elements from the experimental data. The stiffness matrices were then rotated in accordance with the location of their end nodes (centers of vertebral bodies) to align the matrices with the global coordinate system. This procedure is outlined in Panjabi (1973).

Comparison of elastic properties with published data

In order to assess the validity of the mechanical (flexibility) properties of the model, published experiments to determine the flexibilities of the ribs (Schultz *et al.*, 1974a), costo–vertebral and costo–

sternal articulations (Schultz *et al.*, 1974b) and global properties of the thorax (Agostoni *et al.*, 1966; Nahum *et al.*, 1970) were simulated in the complete model or in components of it. The same experimental data were used previously by Andriacchi *et al.* (1974) to validate their model. Based on initial comparisons, the Young's modulus for costal cartilage was changed from 0.30 to 0.48 kN mm^{-2}, and that for the intercostal ligaments from 25 to 5 N mm^{-2} (cross-sectional area of these structures was set at 20 mm^2) to improve the agreements between published data and model prediction.

In the rib experiments (Schultz *et al.*, 1974a), ribs were clamped at one end and loaded by vertical and horizontal loads at the other end. The model deflections in the three principal directions differed by between 1 and 50% from the published values for ribs T2 through T6, with model properties being either more or less flexible than the published measurements. The lower ribs displaced up to five times more than the published experiments. These ribs have long cartilaginous sections anteriorly, which are more ossified in the mature specimens. This probably explained why the model ribs at these lower levels were more flexible.

In the costo–vertebral and costo–sternal experiments (Schultz *et al.*, 1974b), forces were applied to the rib with either the vertebra or the sternum clamped. The model results and the published averages from five subjects were between 1% and 2 times different, with model properties being either more or less flexible than the published measurements.

Tests of the global properties of the thorax (Agostoni *et al.*, 1966; Nahum *et al.*, 1970) involved forces of 100 N applied to compress the rib cages of living subjects in the lateral and antero–posterior directions. Model simulations of these experiments agreed with the mean experimental findings to within 20%, with the finite element model being the less flexible. These agreements with experimental data were considered to be as close as practical, since the nodal data for the model were taken from an adolescent thorax, cross-sectional properties and spinal stiffness matrices were taken from adult data and the experimental flexibility measurements were mostly taken from adult material. The published data showed that there was substantial variability in the adult specimens and subjects tested. There was no available information about how to scale the flexibility data to an individual subject.

Boundary conditions

End constraints were applied to the completed model to provide two alternate boundary conditions which were thought to represent an upper and lower bound of constraints compatible with observed behaviour of the trunk in spinal deformities. In the more constrained model only flexion was permitted at L5 and only flexion and vertical translation were permitted at T1. In the less constrained model, all three rotations were permitted at L5, and only horizontal translations were constrained at T1, to give a minimally constrained model.

Growth and stress-modulated growth

Bony growth in the model was simulated by introducing initial strains. This procedure is analogous to temperature-induced strains commonly used in structural analyses. The ribs are flat bones, and have an unequal distribution of growth along their lengths. In the pig, the growth is greater at the anterior end (Snellman, 1973). Initial strains were therefore varied to produce unequal distribution of growth. Since the general stiffness elements representing intervertebral motion segments did not have geometric or material properties, they were made to expand by computing the appropriate fixed-end-action forces which would produce the required changes in dimensions by elastic deformation, and inputting these directly into the program.

Stresses alter the shape of biological tissues in three different ways: by elastic deformation; by modulation of growth (Bick, 1961; Gooding and Neuhauser, 1965); and by altering turnover and remodelling of mature bone (Carter, 1987; Cowin, 1987). This model incorporated the first two effects only, since it was concerned with the growth spurt when growth predominates. The model was required to represent large shape changes, so recursive running of the program was used to account for geometric nonlinearity. When the model was run recursively, the initial strains for each step could be set to zero. This prevented accumulation of the internal stresses with successive iterations, and thus simulated 'stress relaxation'. An alternative relationship ('stress modulated growth') between initial strain and the level of stress was formulated as

$$\delta\varepsilon = \delta G(1 + \beta\sigma) \tag{1}$$

where $\delta\varepsilon$ = initial strain (%); δG = growth increment (%); σ = stress in material (N mm^{-2}); β = stress sensitivity factor (mm^2 N^{-1}).

In beam elements, the coefficient β introduces variations in growth strain in the tension and compression sides, and hence causes the beam to grow into a curved shape consistent with the strains induced by the local bending moment.

This assumed relationship between growth and stress was incorporated into the model by taking the forces and moments acting on each element at the end of a cycle of computation, calculating the corresponding material stresses and finally deriving the 'fixed end actions' that arise under this stress state when an increment of growth δG is applied. These 'fixed end actions' represent the unbalanced forces for the next step, and were applied as nodal loads in the next cycle of computation.

The fixed end actions in the local coordinate system (where x is the axial direction, y and z represent the principal axis directions of the beam) for a beam

element subjected to a growth increment δG and obeying equation (1) are:

$$\mathrm{FEM_b} = -E\beta\delta G M_b \tag{2a}$$

$$\mathrm{FEF}_{xb} = AE\delta G\left(1+\frac{\beta F_{xe}}{A}\right) \tag{2b}$$

$$\mathrm{FEF}_{yb} = -\frac{E\beta\delta G}{l}(M_b + M_e) \tag{2c}$$

$$\mathrm{FEM_e} = -E\beta\delta G M_e \tag{2d}$$

$$\mathrm{FEF}_{xe} = -AE\delta G\left(1+\frac{\beta F_{xe}}{A}\right) \tag{2e}$$

$$\mathrm{FEF}_{ye} = \frac{E\beta\delta G}{l}(M_b + M_e) \tag{2f}$$

where

$\mathrm{FEM_b}$ = fixed end moment at beginning of beam;
$\mathrm{FEM_e}$ = fixed end moment at end of beam;
FEF_{xb} = fixed end force in x direction at beginning of beam;
FEF_{xe} = fixed end force in x direction at end of beam (etc.);
M_b = moment at beginning of beam at end of previous iteration;
M_e = moment at end of beam at end of previous iteration;
F_{xb} = force in x direction at beginning of beam from previous iteration;
F_{xe} = force in x direction at end of beam from previous iteration (etc.);
A = cross-sectional area of beam;
E = Young's modulus of beam;
l = length of beam.

It was assumed that there was no interaction between forces in the two principal planes of the beam, so the forces in the xz plane were calculated similarly. Torsional forces in the beams and forces in the intervertebral motion segments, and intercostal ligaments were reset to zero at each step, as in the 'stress relaxation' formulation for beams.

Method of solution

Solutions were obtained by the SAP finite element package (Algor SuperSap, Algor Interactive Systems Inc., Pittsburgh PA). In the solution for displacements, linearity of both material properties and geometry (small displacements) were assumed. In order to simulate geometric non-linearity due to large displacements and stress modulated growth, the model was run recursively with increments of growth. After each increment, the nodal geometry was updated by calculated displacements, and new initial strains were set. By varying the incremental step size, the convergence of the recursive solution was established, by ensuring that the computed end point was effectively independent of step size. The complete model had 336 nodes, 2124 equations, and the run time for one solution step was 140 min when run on an AT&T 6300 computer (AT&T, Rolling Meadow, IL) with an 8087 co-processor (Intel, Santa Clara, CA).

Experiments performed with the model

The initial (reference) configuration of the model (Model 1 in Table 1) had average growth of 20%. The rib growth was distributed so that it was four times greater anteriorly than posteriorly (Sneilman, 1973). Also, the growth of the right side was 1.5 times that of the left, which produced 11% greater length of the right rib as compared with the left. These values were adopted because they represent the overall growth during the adolescent growth spurt, and correspond to asymmetry found in patients with thoracic scoliosis in our clinical series (Stokes *et al.*, 1989). The growth was applied in one single linear elastic step in Model 1. The L5 vertebra was constrained in five degrees of freedom: only flexion was permitted. The T1 vertebra was

Table 1. Summary of variations on the model, and the thoracic Cobb angle and maximum vertebral rotation produced

Model No.	Description	Magnitude (apex level) Cobb	Vertebral rotation†
1	(for full description, see text)	3.2° (T6)	0°
2	Free-rotating C.-V.J.*	3.2° (T6)	1.0° (T8)
3	Uniform (but asymmetric) growth along the ribs	2.8° (T6)	0.5° (T4)
4	Intercostal ligaments removed	0.6° (T7)	−0.5° (T8)
5	Minimally constrained model	8.3° (T8)	−1.5° (T10)
6	Minimally constrained model, free-rotating C.-V.J.*	5.6° (T7)	0.5° (T9)
7	5 growth steps of 3.71%, with stress relaxation	3.1° (T6)	0°
8	Stress-modulated growth (10 steps of 1.84%)	2.0° (T7)	0.5° (T9)

*The costo–vertebral joint, at the costo–transverse articulation was released so that it rotated freely as a ball-and-socket joint.

†Positive values signify vertebral axial rotation clockwise from above (posterior elements rotate towards curve concavity).

constrained to prevent horizontal motion, axial rotation and lateral bending. Thus this model represented an individual whose upper thoracic spine remained vertically above the L5 vertebra, and also did not tilt or rotate axially. From this initial configuration, seven alterations of the model were investigated, as shown in Table 1.

The output from each model was examined for: (1) spinal lateral curvature measured by the Cobb method; and (2) vertebral axial rotation.

RESULTS

Asymmetrical growth of the ribs caused lateral deviation and, in most variations of the model, caused axial rotation of the vertebrae. Figs 2 and 3 show the results of Models 2 and 6 respectively, and the results of all models are summarized in Table 1. The general pattern of deformation of the models consisted of thoracic spinal deviation and curvature to the side of the rib cage with the greater growth. In some of the models the spinal deviation was accompanied by axial rotation of the vertebrae in the direction seen clinically: posterior element rotation towards the concavity of the curve, as shown for Model 2 in Fig. 4. The maximum axial rotation of the spine occurred generally a few vertebral levels below the curve apex in those models in which it occurred (Fig. 4).

It was found in the linear elastic model that stresses were highest in the rib elements at their vertebral ends. Therefore, the moments at the costo–transverse connection were released in Model 2 and Model 6 to investigate the effect of permitting free rotation at this location. The ratio between axial rotation and vertebral lateral deviation then increased and was similar to that seen in a clinical population (Stokes *et al.*, 1987).

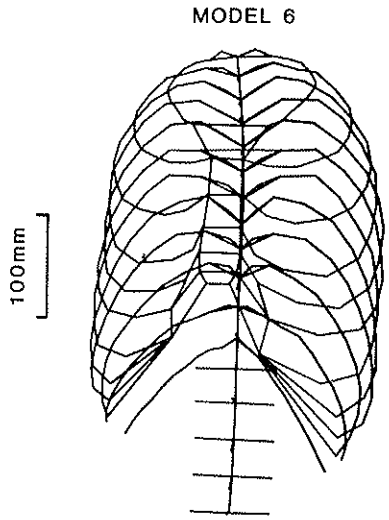

Fig. 3. Back view of the geometric configuration of the initially symmetric model after deformation resulting from average of 20% growth, but distributed so that the ribs and intercostal ligaments 'grew' four times more at the front than the back, and 1.5 times more on the right side than the left. (Model 6 defined in Table 1). This model had six degrees of freedom constrained (minimal constraint), and had moments released at the costo–vertebral joints. It produced a single thoracic curve of 5.6° Cobb. (Intercostal ligaments not shown.)

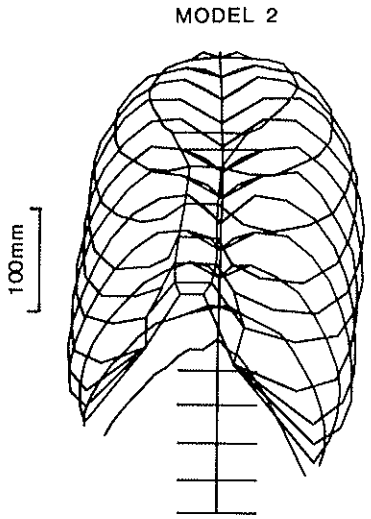

Fig. 2. Back view of the geometric configuration of the initially symmetric model after deformation resulting from average of 20% growth, but distributed so that the ribs and intercostal ligaments 'grew' four times more at the front than the back, and 1.5 times more on the right side than the left. (Model 2 defined in Table 1). This model had moments released at the costo–vertebral joints, and constrained vertebrae at T1 and L5, and generated a small right thoracic and left lumbar scoliosis. (Intercostal ligaments not shown.)

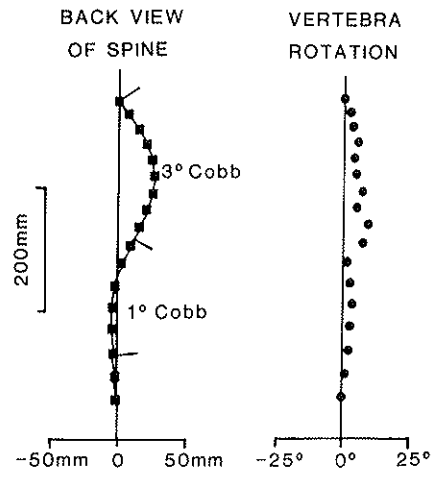

Fig. 4. Plots of the vertebral lateral deviation (left), and of the vertebral axial rotation (right) against the vertical position in the spine, with data from the deformed model shown in Fig. 2. This model had asymmetric growth to produce ribs 11% longer on the right side, and had moments released at the costo–vertebral joints. Note that the horizontal axis for lateral deviations of vertebrae (left graph) has been magnified relative to the vertical axis by a factor of 2, thus exaggerating the scoliosis. In the thoracic region the vertebral rotation is similar to that expected in a spine with scoliosis.

The distribution of growth along each rib was made to be uniform (though still asymmetric between right and left sides) in Model 3. The resulting deformations were found to be affected very little by this variable, but the spinal deformity was slightly less.

The intercostal ligaments were removed in Model 4 to investigate their role. The result was minimal spinal deformation—the deformation remained almost entirely in the asymmetrically growing ribcage.

The importance of the end constraints was investigated in Models 5 and 6, in which the model was minimally constrained: the upper and lower vertebrae could rotate relative to each other about any axis. These models produced greater scoliosis than the constrained models, with a long, single curve pattern, without the compensating lumbar curve (Fig. 2).

In Models 7 and 8, two different stress–growth interactions were investigated. In Model 7, five steps with 3.71% average growth were taken, again for a total (accumulated) growth of 20%. After each step, the node geometry was updated, and all stresses were reset to zero (stress relaxation). In Model 8, 10 steps each averaging 1.84% were taken, and at the end of each step the growth was made to conform with that in equation (1) (stress-modulated growth). With 'stress relaxation' (Model 7) the final configuration of the model was almost identical to Model 1 (within 3%), indicating that these models behaved very linearly, with the deformations dominated by growth strains with minimal elastic strain. With 'stress-modulated growth' (Model 8), the resulting Cobb angle was less than that for the elastic Model 1, but the vertebral rotation was greater and similar to the results for Model 2 in which the costo–vertebral joint moments were released.

DISCUSSION

This study addressed the hypothesis that growth asymmetry produces scoliosis by investigating the effects of asymmetric growth of the rib cage on a model of the thorax. The findings demonstrate the feasibility of this mechanism of initiation of thoracic scoliosis. However, the spinal curves which developed were small in all variations of the model tested, so it appears that some other mechanism must participate in the progression of scoliosis to large curvature during growth. It was anticipated that gravity or muscle forces (omitted from the models reported here) might provide that mechanism. However, a preliminary study of the model with a vertical force applied to the top of the spine, together with asymmetric growth, showed increase in the sagittal spinal curvatures, and not of the scoliosis.

We consider that the presence of vertebral axial rotation together with spinal deviation is an important test of whether a model develops a deformity which truly represents idiopathic scoliosis. In this model such axial rotation was not always present, and when it did occur it usually did not reach a maximal value exactly at the apex of the lateral curve, and did not develop at all in the secondary curves in the lumbar region. The stiffness matrices representing the intervertebral motion segments were taken from published data for the ligamentous thoracic spine, and included off-diagonal 'coupling' terms. The inclusion of these terms did not produce the required axial rotations. Therefore, the missing component actually responsible for development of axial rotation may be the muscles, especially those which cross multiple levels of the spine, or may result from asymmetric development of vertebral bodies due to the altered forces acting on them. In the thoracic region of this model, the costo–vertebral joints and ribs participated in the development of axial rotation. Release of these joints in Models 2 and 6, or the stress modulated growth of the ribs in Model 8, appears to be important for permitting this component of the deformity.

The form and magnitude of spinal curvatures produced by this model depended very much on the end constraints applied. Apparently in reality there is some subtle balancing of the trunk, dependent on spinal proprioception and balance, fine tuning of muscle forces and tissue remodelling and growth which are only represented very crudely by the end constraints incorporated in this model.

The stress-modulated growth formulation used here was linear, and was probably a great oversimplification of the real interaction between stress and growth of bone. It was found that if the constant β became too great the model was unstable, apparently because successive iterations produced increasing, accumulating stresses within this statically indeterminate structure. In the stress modulated growth model (Model 8), the value of β was 10^{-2} mm^2 N.$^{-1}$ This was close to the maximum value of β at which the model remained stable. The factors which control growth of ribs (which are flat bones) as well as other bones are poorly understood, but models such as this one help to show which formulations are feasible.

The model formulation is considered to be an improvement over previous models (Andriacchi *et al.*, 1974; Sundaram and Feng, 1977; Roberts and Chen, 1970) because of improvements in geometric (shape) data, incorporation of bone growth and of published data from experimental measurements of three-dimensional flexibility of component parts. A recursive method of updating the geometry was developed to account for geometric non-linearities, and to permit incorporation of 'stress-modulated growth'. The model also takes advantage of developments in computation techniques, permitting the solutions to be obtained from programs running in a personal computer.

The model developed here may also be used to study correction of scoliosis deformity, by incorporating the actual geometry of a patient into the model node list and applying forces to simulate those occur-

ring in surgery or brace treatment, thus individualizing the kind of pre-treatment simulations done previously (Schultz *et al.*, 1981; Patwardhan *et al.*, 1986; Subbaraj *et al.*, 1989). The main problem in such analyses is to obtain the correct material properties to match those of each patient.

This study simulated asymmetric growth of the ribs, and not of the vertebrae. Previously, abnormal growth of vertebrae has been implicated in the etiology of scoliosis (Roaf, 1963; Dickson *et al.*, 1984). If the growth asymmetries of the ribs in these simulations were also applied to the vertebrae, a large scoliosis would develop. A 10% length difference between right and left sides of vertebrae having a width of 30 mm gives a radius of curvature of the spine of 300 mm. Normelli *et al.* (1985) and Agadir *et al.* (1988) emphasized rib cage development in the etiology of scoliosis in their clinical studies and in an animal model. Many abnormalities, including asymmetries of connective tissue, neurologic behavior and growth variables have been observed in patients with idiopathic scoliosis (Nachemson and Sahlstrand, 1977) but it is very difficult to determine which mechanisms are responsible for development of the deformity and to distinguish between primary (causative) and secondary asymmetries. The exact cause of idiopathic scoliosis remains unknown. Determining the cause will probably require a greater understanding of the normal growth and development of the musculoskeletal system.

Acknowledgements—This work was supported by NIH RO1 AR 38507. It was done with the assistance of Jean Dansereau, Sylvia Most, Hong Rong and Mack Gardner-Morse.

REFERENCES

Agadir, M., Sevastik, B., Sevastik, J. A., Persson, A. and Isberg, B. (1988) Induction of scoliosis in the growing rabbit by unilateral rib-growth stimulation. *Spine* **13,** 1065–1069.

Agostoni, E., Mognoni, G., Torri, G. and Miserocchi, G. (1966) Forces deforming the rib cage. *Respir. Physiol.* **2,** 105–117.

Andriacchi, T., Schultz, A., Belytschko, T. and Galante, J. (1974) A model for studies of mechanical interactions between the human spine and rib cage. *J. Biomechanics* **7,** 497–507.

Bick, E. M. (1961) Vertebral growth: its relation to spinal abnormalities in children. *Clin. Orthop.* **21,** 43–48.

Carter, D. R. (1987) Mechanical loading history and skeletal biology. *J. Biomechanics* **20,** 1095–1109.

Cowin, S. C. (1987) Bone remodeling of diaphyseal surfaces by torsional loads: theoretical predictions. *J. Biomechanics* **20,** 1111–1120.

Dangerfield, P. H., Burwell, R. G. and Vernon, C. L. (1980) Anthropometry and scoliosis. In *Spinal Deformities* (Edited by Roaf, R.), pp. 259–280. Pitman, U.K.

Dansereau, J. and Stokes, I. A. F. (1988) Measurements of the three-dimensional shape of the rib cage. *J. Biomechanics* **21,** 893–901.

Dickson, R. A., Lawton, J. O., Archer, I. A. and Butt, W. P. (1984) The pathogenesis of idiopathic scoliosis. Biplanar spinal asymmetry. *J. Bone Jt Surg.* **66B,** 8–15.

Fung (1981) *Biomechanics. Mechanical Properties of Living Tissues*, pp. 197–202. Springer, New York.

Gloobe, H. and Nathan, H. (1970) The costovertebral joint. Anatomical observations in various mammals. *Anat. Anz.* **127,** 22–31.

Gooding, C. A. and Neuhauser, E. B. D. (1965) Growth and development of the vertebral body in the presence and absence of normal stress. *Am. J. Roentg.* **93,** 388–394.

Jordanoglou, J. (1969) Rib movement in health, kyphoscoliosis, and ankylosing spondylitis. *Thorax* **24,** 407–414.

Nachemson, A. and Sahlstrand, T. (1977) Etiologic factors in adolescent idiopathic scoliosis. *Spine* **2,** 176–184.

Nahum, A. M., Gadd, C. W., Schneider, D. C. and Kroell, C. K. (1970) (cited in Andriacchi *et al.*, 1974).

Normelli, H., Sevastik, J. and Akrivos, J. (1985) The length and ash weight of the ribs of normal and scoliotic persons. *Spine* **10,** 590–592.

Panjabi, M. M. (1973) Three-dimensional mathematical model of the human spine structure. *J. Biomechanics* **6,** 671–680.

Panjabi, M. M., Brand, R. A. and White, A. A. (1976) Three-dimensional flexibility and stiffness properties of the human thoracic spine. *J. Biomechanics* **9,** 185–192.

Patwardhan, A. G., Bunch, W. H., Meade, K. P., Vanderby, R. and Knight, G. W. (1986) A biomechanical analog of curve progression and orthotic stabilization in idiopathic scoliosis. *J. Biomechanics* **19,** 103–117.

Roaf, R. (1963) The treatment of progressive scoliosis by unilateral growth-arrest. *J. Bone Jt Surg.* **45B,** 637–651.

Roberts, S. B. and Chen, P. H. (1970) Elastostatic analysis of the human thoracic skeleton. *J. Biomechanics* **3,** 527–545.

Roberts, S. B. and Chen, P. H. (1972) Global geometric characteristics of typical human ribs. *J. Biomechanics* **5,** 191–201.

Schultz, A. B., Benson, D. R. and Hirsch, C. (1974a) Force–deformation properties of human ribs. *J. Biomechanics* **7,** 303–309.

Schultz, A. B., Benson, D. R. and Hirsch, C. (1974b) Force–deformation properties of human costo–sternal and costo–vertebral articulations. *J. Biomechanics* **7,** 311–318.

Schultz, A., Haderspeck, K. and Takashima, S. (1981) Correction of scoliosis by muscle stimulation. Biomechanical analyses. *Spine* **6,** 468–476.

Snellman, O. (1973) Growth and remodelling of the ribs in normal and scoliotic pigs. *Acta orthop. scand.* **149,** 28–41.

Stokes, I. A. F., Bigalow, L. C. and Moreland, M. S. (1987) Three-dimensional spinal curvature in idiopathic scoliosis. *J. Orthop. Res.* **5,** 102–113.

Stokes, I. A. F., Dansereau J. and Moreland, M. S. (1989) Rib cage asymmetry in idiopathic scoliosis. *J. orthop. Res.* **7,** 599–606.

Subbaraj, K., Ghista, D. N. and Viviani, G. R. (1989) Presurgical finite element simulation of scoliosis correction. *J. biomed. Engng* **11,** 9–18.

Sundaram, S. H. and Feng, C. C. (1977) Finite element analysis of the human thorax *J. Biomechanics* **10,** 505–516.

Weinstein, S. L. and Ponseti, I. V. (1983) Curve progression in idiopathic scoliosis. *J. Bone Jt Surg.* **65A,** 447–455.